



Cite this: *Analyst*, 2021, **146**, 3177

# Inkjet-printed O<sub>2</sub> gas sensors in intelligent packaging†

M. D. Fernández-Ramos,<sup>ib</sup> \*<sup>a,b</sup> M. Pageo-Cabrera,<sup>a</sup> L. F. Capitán-Vallvey<sup>ib</sup> <sup>a,b</sup> and I. M. Pérez de Vargas-Sansalvador<sup>a,b</sup>

An inkjet printed membrane is presented as a colorimetric sensor for oxygen for use in smart packaging, in order to quickly inform the consumer about possible degradation reactions in modified atmosphere products (MAP). The colorimetric sensor is based on the redox dye, toluidine blue (TB), a sacrificial electron donor, glycerol, and, hydroxypropyl methylcellulose, as the hydrophilic polymeric matrix. The UVC-wavelength activated TB is photoreduced by SnO<sub>2</sub> nanoparticle ink. This colorimetric oxygen indicator stays colourless upon exposure in nitrogen atmosphere to 7 min UVC light (6 W·cm<sup>-2</sup>). The photoreduced TB to leuco TB recovers its original colour upon exposure to oxygen for 55 min under ambient conditions (~21 °C, ~55%RH, 21% O<sub>2</sub>). The characteristics of the sensor have been evaluated, including its functionality through the colorimetric response to different oxygen concentrations as well as the influence of experimental variables such as humidity and temperature using a digital camera as the detector. The results obtained show that: (1) the colorimetric sensor remains stable in the absence of oxygen; (2) relative humidity greater than 60% significantly affects the reoxidation process; and (3) the temperature has a significant influence on the colour recovery, although the stability increases considerably when the sensor is kept refrigerated at 4 °C. A real application to packaged ham was performed, demonstrating that the printed colorimetric sensor is stable for at least 48 hours once activated and when the container deteriorates upon the entrance of oxygen, the sensor returns to its original blue colour, demonstrating its utility as a UVC-activated colorimetric oxygen sensor.

Received 17th February 2021,

Accepted 26th March 2021

DOI: 10.1039/d1an00295c

[rsc.li/analyst](http://rsc.li/analyst)

## 1. Introduction

Food companies are increasingly interested in controlling the shelf life of food to preserve the health of consumers and to reduce food waste. Shelf life is the result of the relationship between food quality, consumer acceptability and packaging performance. For this reason, research in the field of food is currently very active, primarily in packaging, so as to help consumers make a more conscious and safer purchase.

The main objective of this study is to find a method to analyse packaged food that does not require opening the package. Hence intelligent packaging, which has the function of monitoring variations in the product and responding directly to them by changing a physical or chemical property. This has enormous potential to improve the safety, quality and traceability of food products, as well as increasing consumer

convenience. This is achieved by including an indicator system inside the food package. Ideally, these indicators should be a simple colorimetric sensor that can be evaluated with the naked eye by unqualified personnel, non-toxic and directly integrated into the package.<sup>1</sup>

Oxygen indicators are the most common gas indicator for food packaging applications because the presence of oxygen in the package helps microorganisms to proliferate, spoiling food. For this reason, the packaging of food either in vacuum<sup>2</sup> or in a modified atmosphere (MAP) using nitrogen or carbon dioxide<sup>3,4</sup> helps the food to stay fresh for longer than if stored directly in the air. Therefore, the use of economic indicators for oxygen inside packaging can provide a quality guarantee to the consumer.<sup>5</sup>

Current colorimetric oxygen indicators are based on some of the following three principles:<sup>6</sup> (1) an oxygen binding reaction; deoxyhemoglobin converting to oxyhemoglobin was one of the first reported colorimetric indicators of oxygen,<sup>7</sup> but it is not very stable, lasting only two days at room temperature. Another example uses myoglobin encapsulated in a sol-gel glass matrix,<sup>8</sup> although it also has storage problems in addition to a weak colour change. Another sensor described is based on synthetic metal complexes that bind to oxygen such

<sup>a</sup>ECsens, Department of Analytical Chemistry, University of Granada, Granada 18071, Spain. E-mail: [mdframos@ugr.es](mailto:mdframos@ugr.es)

<sup>b</sup>Unit of Excellence in Chemistry applied to Biomedicine and the Environment of the University of Granada, Spain

†Electronic supplementary information (ESI) available. See DOI: 10.1039/d1an00295c



as bis (histidinate) cobalt,<sup>9,10</sup> although it has poor colour change and sensitivity to external factors such as pH and humidity; (2) the second principle involves a redox reaction or light-activated redox reaction, with the most popular being the Ageless Eye® produced by the Mitsubishi Gas company to support its wide range of oxygen scavengers.<sup>10</sup> Typically, it comprises a redox dye, methylene blue (MB), a strong reducing agent, glycosides, and a redox dye, Acid Red 52, that changes from purple to pink when the ambient gas is at oxygen levels  $\leq 0.1\%$  and turns purple when the atmosphere is  $\geq 5\%$  oxygen. Its disadvantages include its high cost and the need for storage in an anaerobic atmosphere; and (3) colorimetric redox dye light activated by a sacrificial electron donor. For example, the riboflavin/EDTA photosystem has been reported together with methylene blue as an UV/Vis activated colorimetric indicator. Its blue colour in air becomes colourless in the absence of oxygen.<sup>11</sup> A considerable variety of this type of sensor has been developed, all based on a redox dye, typically methylene blue (MB), a sacrificial electron donor (SED) and a UV light sensitive semiconductor photocatalyst (SC), all encapsulated within a polymer.<sup>12–19</sup> When the sensor is exposed to UV light, electrons are promoted from the valence to the conduction band within the SC to create electron hole pairs. The SED is then oxidized by reaction with the photogenerated holes, leaving the photogenerated electrons free to reduce the redox dye to its reduced colourless form. Upon exposure to oxygen, the redox dye is oxidized back to its blue form.

Some of the basic components in the proposed sensors in the bibliography have been modified, trying to improve their properties, although they all share the use of titanium oxide nanoparticles, which makes UVA light necessary to activate the sensor. The drawback is that the most common visible light fluorescent tubes used in supermarkets have an emission peak in the UVA region (typically at 365 nm), allowing the indicator to be reactivated uncontrollably. This disadvantage has been solved by replacing them with tin oxide nanoparticles that are not activated by this type of UV radiation.<sup>15</sup> Other alternatives to using traditional methylene blue as a redox dye in UV-activated O<sub>2</sub> indicators have also been tested, such as the anthraquinonic dye Remazol brilliant blue R encapsulated in an ink containing a polymer, glycerol and TiO<sub>2</sub> as the UV-activated semiconductor photocatalyst;<sup>20</sup> and thionine, glycerol and P25 TiO<sub>2</sub> and the prolamine protein zein as polymer.<sup>18</sup> This was the first UV-activated oxygen indicator film to use alginate as a coating polymer, which decreased the leaching of the dye due to insoluble complex formed. Many attempts have been made to improve the characteristic of the TiO<sub>2</sub>-based system, such as the use of platinum catalysts loaded onto the SC to control the response time, reducing the recovery time,<sup>16</sup> and the use of graphene oxide wrapped TiO<sub>2</sub> nanoparticles as the UV-activated colorimetric oxygen sensor.<sup>17</sup>

In order to find the best integration of the sensor in packaged food, a good alternative to this sensor involves printing the sensor directly on the container. Efforts have also been made in this regard, including the development of an MB and dodecyl sulphate ionic pair, producing an oxygen sensitive ink

that can be printed on films or packages of different hydrophobic polymers,<sup>14</sup> although its viability was not proven. An initial approach to obtaining a smart oxygen sensor directly on the plastic material that makes up the package uses MB as the dye redox, DL-threitol as the sacrificial electron donor, together with TiO<sub>2</sub> as the semiconductor, extruded in low density polyethylene.<sup>21,22</sup>

To achieve intelligent packaging, the indicator film must be deposited, if possible, on the material that forms the food container. Among other techniques, inkjet printing is becoming increasingly popular in the packaging industry<sup>23</sup> to print directly on packages because it is a simple and environmentally-friendly system and it is compatible with many substrates. In this line, a printed sensor based on colloidal TiO<sub>2</sub> particles has been developed by Mills *et al.* to obtain a water-based UV-activated oxygen ink by a drop-on-demand inkjet printer which does not contain a resin; instead titanium is mixed with MB and tartaric acid.<sup>22</sup>

This study describes a colorimetric oxygen ink that is directly printed by ink jetting on packaging formed by tin(IV) oxide nanoparticle ink, toluidine blue (TB), glycerol and hydroxypropyl methylcellulose (HPMC) prepared using water as the solvent to create a UVC-activated O<sub>2</sub>-sensitive smart sensor for applications in the agro-food industry.

## 2. Experimental section

### 2.1. Reagents and materials

Hydroxypropyl methylcellulose (HPMC, Methocel E-5, LV USP/EP premium grade) (Dow Chemical Iberia S.L., Tarragona, Spain) was used as the membrane polymer. The reagents toluidine blue (TB), resorufin, 2,6-dichloroindophenol sodium salt hydrate, methylene blue, glycerol and tin(IV) oxide nanoparticles ink in butanol 2.5 wt%, viscosity 3.5 cP, were all obtained from Sigma-Aldrich (Madrid, Spain). Sheets of Mylar-type polyester from Goodfellow (Cambridge, UK) were used as support for the membranes. Vacuum bags, 180 × 300 mm, came from Sierra Nevada Compost and Paper S.L., Granada (Spain) and the heat sealer PFS-300 mm electric impulse sealing machine from Barcelona (Spain). Ham samples were bought from the Mariscal butcher shop, Granada (Spain).

Inks were characterized using viscometer Visco Basic Plus (Fungilab, Barcelona, Spain) and surface tensiometer Theta Lite Attension (Biolin Scientific AB, Stockholm, Sweden). In order to activate the oxygen sensing membranes, a UVC lamp VL-6MC 6 W was used for  $\lambda = 254$  nm; a UVB lamp 6W for  $\lambda = 312$  nm from Vilber (Vilber Lourmat Deutschland GmbH, Eberhardzell, Germany) and a UVA lamp Sylvania Black Light F15 W/350BL-TB (×2)  $\lambda = 350$  nm, power 30 W (×2) (Feilo Sylvania Group, Budapest, Hungary).

The standard gaseous mixtures to characterize the membranes were prepared using N<sub>2</sub> as the diluting gas, controlling the flow rates of the high purity O<sub>2</sub> and N<sub>2</sub> gases that enter the mixing chamber with computer-controlled mass flow controllers (Air Liquide España S.A., Madrid, Spain). The system



works at a total pressure of 760 Torr and a flow rate of 500 cm<sup>3</sup> min<sup>-1</sup>. To produce different humidity conditions (from 17 to 100% RH), a Controlled Evaporator Mixer system (CEM) was used. It consists of a mass flow controller for the measurement and control of the carrier gas flow (N<sub>2</sub> gas) and a mass flow meter for liquids (MiniCoriflow) with a range of 0.4–20 g h<sup>-1</sup> of liquid (water in this case). A 3-way EMC mixing valve and an evaporator controls the liquid flow and the mixing of the liquid with the carrier gas flow. In addition, it contains a temperature-controlled heat exchanger to heat the mixture and completely evaporate the liquid (100 °C for water).

## 2.2. Preparation of inkjet-printed oxygen sensing membrane

The oxygen sensing membranes were printed with a Fujifilm Dimatix DMP-2831 printer (Fujifilm Dimatix, Inc., Santa Clara, CA, USA), using cartridges with 16 nozzles and a nominal droplet size of 10 pL. Print designs were made using the pattern editor in the Dimatix Drop Manager software. Sensing membranes were printed on thermoplastic polyester sheets of Mylar-type polyester from Goodfellow (Cambridge, UK) after carefully cleaning the plastic surface with ethanol. The membranes were printed in a circular shape and the printing process (12 pL) was repeated four times – after allowing them to dry each time – for the same membrane in order to obtain homogeneous and deep blue membranes, such that the colour change could be well perceived.

This ink has rheological properties adjusted to the requirements of the printer, namely: 10–12 cPs viscosity; 28–33 dynes per cm surface tension; <100 °C boiling point; >1 g cm<sup>-3</sup> density; <0.2 µm particle size; 4–9 pH. The characteristics of the prepared ink were: pH 4.1; viscosity 10 cP and surface tension 28 dynes per cm. The prepared inks were degassed after use by means of an ultrasonic bath to prevent dissolved gas, which inhibits jetting. Before filling the cartridge, the inks were filtered through a 0.2 µm filter and then maintained under vacuum for almost two hours after use for optimal jetting.

Parameters like substrate, print head temperature, drop spacing, print head height and print design are important to obtain a printed sensor. Temperature is also a significant variable when more than one layer is printed, as is the case when four layers are printed. The optimum temperature for printing was 45 °C. This temperature helped the drying process. Moreover, with temperatures above 45 °C, no appreciable improvement in the results is observed. A drop spacing of 30 µm was employed, as this achieved a high-quality film while using a minimum volume of ink. A print head height of 1.7 mm was selected to print on the plastic substrate, producing a circular shape of 1 cm in diameter with an average film thickness around of 40 nm.

## 2.3 Image capture, processing and sensing scheme

The change in colour of the sensing membranes from colourless to blue in the presence of gaseous oxygen was recorded with a Canon PowerShot G12 digital camera (Canon Inc., Tokyo, Japan). The optimized setting conditions used to photo-

graph the membrane were: macro, ISO 100, shutter speed 1/500 s, aperture value f/4 and focal length of 6.1 mm. To keep all the image-gathering conditions the same, a homemade wooden enclosure<sup>24</sup> was used. The camera was placed in the front of the box with two LED 6500 K lamps placed at 45° with respect to the digital camera, with the membrane in a fixed position inside the box to isolate it from external radiation, a position that was maintained constant for all the experiments.

To evaluate the colour change of the printed sensor, a photograph was taken in JPEG format.

RGB and HSV colour coordinates were obtained from the region of interest (ROI) of the digitized membrane using Image J software (National Institutes of Health).

The colour coordinates of HSV and RGB colour spaces were obtained along with the Colour Space Converter plugin to generate the median values of each colour coordinate from the pixels (around 160 000) that compose the ROI as the area of the digitalised membrane selected to perform the colorimetric analysis in order to get analytical information.

## 2.4. Sensor response evaluation

In order to evaluate the response of the printed membrane to oxygen, previous activation of the printed membrane is required. Therefore, different printed membranes were prepared and exposed to different types of UV lamps, UVA, UVB and UVC, with different powers of UV radiation, also establishing the optimal distance between the membrane of the printed sensor and the source of the UV radiation. Another parameter that was evaluated to select the optimal composition of the printed membranes is the time it takes for the printed membrane to respond when exposed to atmospheric oxygen.

# 3. Results and discussion

## 3.1. Optimization of sensitive ink

The UV-activated O<sub>2</sub> sensitive ink is formed by a redox dye that varies in sensitivity, depending on the characteristics of the dye used. Phenothiazinic methylene blue is the most popular redox dye used to be photoreduced by TiO<sub>2</sub> and/or SnO<sub>2</sub>, to sense oxygen, due to its intense colour ( $\epsilon = 82.000 \text{ M}^{-1} \text{ cm}^{-1}$ ;  $E^\circ = 0.5 \text{ V}$ ), good stability and low price.<sup>25</sup> Alternatively, other dyes has been proposed such as toluidine blue<sup>26</sup> ( $E^\circ = 0.488 \text{ V}$  and  $\epsilon = 51.000 \text{ M}^{-1} \text{ cm}^{-1}$ ) and oxazone resorufin<sup>27</sup> ( $E^\circ = 0.34 \text{ V}$  and  $\epsilon = 65.000 \text{ M}^{-1} \text{ cm}^{-1}$ ), as well as 2,6-dichloroindophenol sodium salt hydrate<sup>28</sup> ( $E^\circ = 0.66 \text{ V}$  and  $\epsilon = 17.400 \text{ M}^{-1} \text{ cm}^{-1}$ ). In this respect, four redox dyes were tested in addition to methylene blue, toluidine blue, resorufin and 2,6-dichloroindophenol sodium salt hydrate.

Different sensor films were prepared using 20 µL of the sensing cocktail with the following composition: 2% w/v HPMC in water as solvent, 0.7% w/v glycerol, 0.05%w/v of each of the redox dyes and 0.17%w/v tin(IV) oxide nanoparticle ink in butanol. The blue membranes were activated using UVB light for 90 min, becoming colourless. After the activation, the



sensors were exposed to atmospheric conditions to check their response to oxygen. The sensor containing the redox dye 2,6-dichloroindophenol sodium salt hydrate did not present any response to oxygen. As this dye is photosensitive, light can affect its response. The response obtained using resorufin was very low, in addition to presenting a very high activation time. Methylene blue and toluidine blue responded well and quickly to oxygen. Methylene blue, used as redox dye in this type of sensor, has a redox potential of 0.5 V, but this redox dye can be replaced by another redox dye with a less positive redox potential than MB, creating more sensitive UV activated oxygen indicators.<sup>29</sup> As a result, toluidine blue ( $E^\circ = 0.48$  V) was selected as a redox dye to evaluate its potential use in this type of sensor. In order to optimise the activation process of the sensor, three different UV lamps were used (UVA, UVB and UVC). Table 1 shows the results obtained with each lamp, showing that the UVA lamp did not activate the sensor. The UVB and UVC lamps were capable of activating the membranes, but the UVB required more time than the UVC, which is why UVC was selected for further experiments. This result is consistent with the bandgap value of the semiconductor used. In our case the bandgap for  $\text{SnO}_2$  is 3.67 eV, which means that a higher energy must be given than that bandgap, in this case, greater than the energy equivalent to 337.8 nm (which is the energy provided by that wavelength). In the absence on  $\text{SnO}_2$  the dye does not bleach, besides at 254 nm (UVC) the dye will absorb strongly, but less so than at 312 nm and even less so at 365 nm, thus, the dye will screen the  $\text{SnO}_2$  and also be electronically excited. UVC exposure will bleach the dye and UVC/dye plus glycerol may cause it reversible bleaching.

Fig. 1 show the colour change of this sensor, before UV irradiation (A), immediately after irradiation (B) and when exposed to atmospheric oxygen (C).

Once the activation step was optimised, the selection of the analytical parameter was studied. After the membranes were

activated, photographs were taken under the above mentioned conditions until the membranes completely recovered their colour under ambient oxygen. The coordinates from the RGB and HSV colour spaces were studied, obtaining the response observed in Fig. S1 (ESI†).

As can be seen, the G, B, S and V coordinates did not respond to oxygen, since no variations were observed when exposed to ambient oxygen. The R and H coordinates, on the contrary, changed their value in the presence of oxygen. Of these two parameters, H was selected as analytical parameter to quantification of oxygen in this sensor, since the variation it causes is much greater than when using the R coordinate and it is more sensitive against oxygen variations in the membrane.

Given the intended application, short activation times and rapid response to oxygen are required. Therefore, the amounts of different components of the sensitive ink were optimised. Glycerol was tested from 0.7 to 2% w/v, showing that the higher the amount of glycerol, the higher the activation time and the response to oxygen. According to the results presented in Table 2, the use of the minimum amount of glycerol results in a shorter activation time and the fastest response. Thus, 0.7% w/v was the amount selected for the preparation of the sensitive ink. Smaller quantities of glycerol were not tested because they are difficult to handle due to their viscosity.

In order to optimise the concentration of tin(IV) oxide nanoparticles, different inks were prepared from 0.01 to 0.13% w/v. The maximum response speed and minimum activation time was obtained with 0.02% w/v, which was selected as the optimum concentration (Table 3).

### 3.2. Analytical characterization of the sensing membranes

The influence of the oxygen concentration was studied by subjecting the activated sensor to different concentrations of oxygen. After 10 min of contact with each oxygen concentration and the sensor, a photograph was taken (Fig. 2 presents the results), showing that it is possible to use this sensor to

**Table 1** Characteristics of different UV lights tested on oxygen gas membrane

Type of light	$\lambda$ (nm)	Power (W)	Irradiance ( $\text{mW cm}^{-2}$ )	Activation	Activation time (min)
UVA	350	45	15	No	180
UVB	312	6	6	Yes	115
UVC	254	6	6	Yes	55

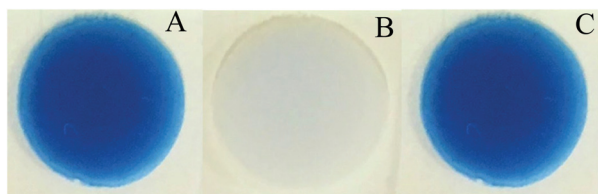


**Fig. 1** Images of the printed sensor: (A) before UVA irradiation; (B) immediately after irradiation; and (C) sometime after exposure to oxygen (in air) when it has fully recovered its original colour.

**Table 2** Optimization of glycerol amount

Glycerol (%w/v)	Activation time (min)	Response speed ( $\text{min}^{-1}$ )	Recovery time (min)
0.7	55	0.0097	82
0.9	55	0.0060	136
1.3	55	0.0125	92
2.0	100	0.0208	46

**Table 3**  $\text{SnO}_2$  ink nanoparticle optimization

Nanoparticles $\text{SnO}_2$ (%w/v)	Activation time (min)	Response speed ( $\text{min}^{-1}$ )	Recovery time (min)
0.01	45	0.0065	53
0.02	46	0.0115	58
0.05	47	0.0125	79
0.10	55	0.0297	82
0.13	65	0.0398	94



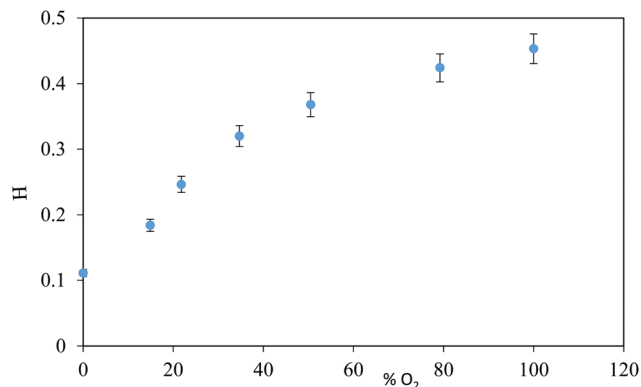


Fig. 2 Sensor response to O<sub>2</sub>.

provide a quantitative measurement of the ambient oxygen level.

In intelligent packaging, there are two important factors to take into account: temperature and relative humidity. The influence of the temperature is an important factor because a great number of foods are stored at low temperatures. This was evaluated monitoring the recovery profiles after photoactivation at 4 °C, 7 °C and 21 °C, introducing the sensor into a thermal camera, which is filled with 21% oxygen (atmospheric concentration) and 55% RH, taking images at controlled time intervals. This study indicates at 21 °C, the sensor recovered its colour in approximately 55 min, while at 4 °C it took more than a 1 day, so this sensor has potential for use in food packaging as a possible indicator of perishable foods that can be kept in the refrigerator for a limited time before consumption. These results match previous studies found in literature (see Fig. 3A),<sup>22</sup> where a temperature drop extended the indicator's recovery.

To study the influence of humidity, the photoactivated indicator was monitored under different % RH, taking a photo-

graph after 10 min exposure at each RH studied. Fig. 3(B) shows the results obtained, with a linear dependence with the rate increasing by 2.2 times over the RH range 10–100%. The results are in accordance with the bibliography when glycerol is also used,<sup>22</sup> since water may have a plasticizing action on the glycerol at high RH due to its hygroscopic nature.<sup>16</sup>

To find out whether the sensor could be reused, a photoactivated sensor was left in contact with ambient air, following the response by taking photographs periodically. Once the sensor fully recovered its initial colour, it was photoactivated again, performing the same process as seen in Fig. 4. However, the signal did not return to its initial value after oxidation, the signal decrease slightly with increasing cycles in air and even with the sixth photoactivation, the sensor is considerably less bleached, meaning that there is not a completely reversible photobleaching of the dye and there is generation of reaction products in the ink film.

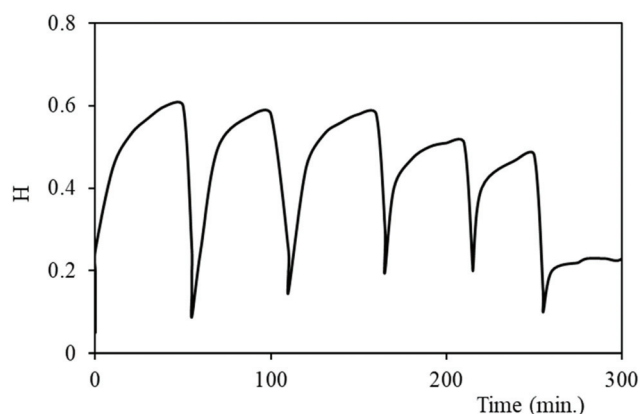


Fig. 4 Regeneration of oxygen indicator: H coordinate versus activation cycles.

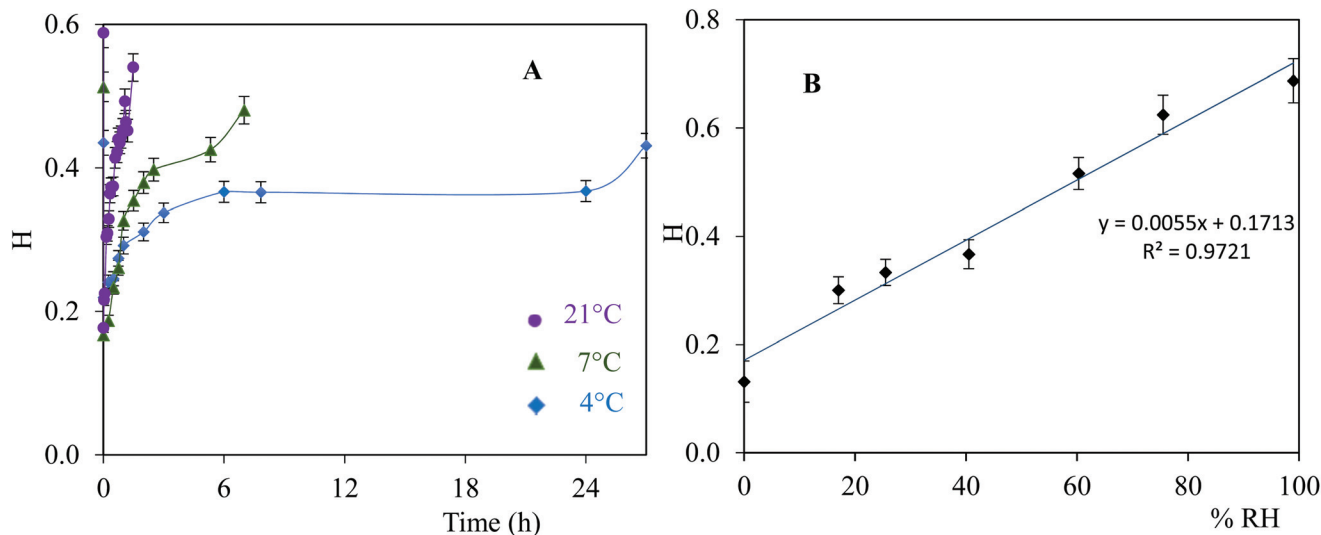


Fig. 3 Influence of sensor response to experimental variables: (A) influence of temperature; and (B) influence of % RH.



**Table 4** Comparison of the analytical characteristics of UV light photoactivated optical sensors

Redox dye	Semiconductor	Other components	Activation time (min)	Reoxidation time (min)	Ref.
MB	SnO <sub>2</sub>	HEC/glycerol	1.66	5	15
MB	TiO <sub>2</sub>	PE/treitol	<1.5	540	21
MB	TiO <sub>2</sub>	Tartaric acid	3	720	22
MB	TiO <sub>2</sub>	Acrylate/BKD	40	11 520	31
Thionine	TiO <sub>2</sub>	Z/A/glycerol	5	240	18
MB	TiO <sub>2</sub>	PS/glycerol	<1	720	32
MB	TiO <sub>2</sub>	Carrageenan/glycerol	4	480	19
RBBR	TiO <sub>2</sub>	HEC/glycerol	4	1440	20
TB	Ink SnO <sub>2</sub>	HPMC/glycerol	7	2160	Current study

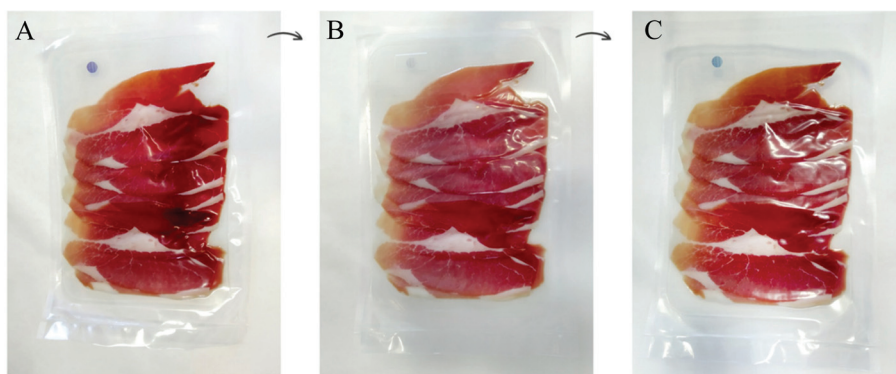
MB: Methylene blue; TB: Toluidine blue; HEC: Hydroxyethyl cellulose; PS: Polystyrene; PE: Polyethylene; BKD: Benzyl dimethyl ketal; Z: Zein; A: Alginates; HEC: Hydroxyethyl cellulose; RBBR: Remazol brilliant blue.

Table 4 shows a comparison of activation and reoxidation times of the different oxygen indicators proposed in the bibliography. If low activation and response times are desired, the amount of glycerol must be lower.<sup>21</sup> In general, the activation time is usually quicker than in our case, but the reoxidation time is very similar.

With a few exceptions,<sup>19,20</sup> methylene blue is undoubtedly the most widely used redox dye in this type of sensor. On the other hand, the semiconductor most commonly used in the bibliography is TiO<sub>2</sub>,<sup>14</sup> although it has the disadvantage of possible activation with UVA light from lamps in the supermarket. As this study uses a nanoparticulate SnO<sub>2</sub> ink, this problem is avoided. The activation time depends on the power of the lamp used, which is quite varied: UVB,<sup>15</sup> UVA light,<sup>16,21,22,30</sup> or the UVC light used previously on carrageenan-coated films.<sup>19</sup> In the present study, 6 W UVC light was used. The reoxidation time of the dye after it comes into contact with O<sub>2</sub> is the most variable. This may be due to the gas oxygen permeability of the film formed with the sensor.<sup>29</sup> In addition, of all the sensors in Table 4, only the one developed here and the one using tartaric acid, MB and TiO<sub>2</sub> as the sacrificial electron donor, redox dye and semiconductor, respectively<sup>22</sup> were printed by inkjet. The sensor proposed in

this study can be printed directly onto the container, allowing it to be developed at the industrial level, since production costs are reduced. It also has a good response when kept at 4 °C. The approximate price of each printed sensor would be  $9 \times 10^{-4}$  euros, per unit. Batch production would further lower the final price.

Finally, a possible real use for this type of oxygen indicator in food packaging was tested. 10 samples of fresh uncooked ham were packaged under N<sub>2</sub> atmosphere and sealed with the oxygen sensor inside. The sensor was activated inside the container and remained stable without showing any colour change. The colour was monitored for one week, observing a dispersion of around 5%, within the dispersion obtained in its preparation. The response was evaluated once the container was opened and exposed to the external oxygen atmosphere. At that time, the evolution of the colour in all the containers was similar, all having the same maximum reference value, coinciding with the maximum intensity of the sensor colour that indicated the end of the useful life of the food. At present, there appears to be no obvious long-term stability issues with this indicator in its activated or deactivated form for at least 48 hours (Fig. 5).



**Fig. 5** Photographs of UVA-activated oxygen indicator placed inside a plastic package flushed with CO<sub>2</sub> and sealed: (A) the package is recently sealed and the indicator is blue; (B) the indicator has been bleached by a UVC light burst, the indicator inside remains bleached for 48 h; and (C) upon opening the package, the entrance of oxygen causes the indicator to recover its original colour.



## 4. Conclusion

An inkjet-printed oxygen sensor was developed for use in smart packaging to quickly inform the consumer of the possible degradation reactions of packaged food in modified atmosphere (MAP). The sensor is based on a redox dye toluidine blue (TB), a sacrificial electron donor, glycerol and hydroxypropyl methylcellulose as hydrophilic polymeric matrix and activated UVC. The TB is photoreduced by SnO<sub>2</sub> nanoparticle ink. This oxygen indicator ink is inkjet-printed onto a plastic film and in the absence of oxygen, the film stays bleached upon exposure to 7 min of UVC light (6 mW cm<sup>-2</sup>). In this way, the TB indicator is photoreduced to leuco toluidine blue and recovers its original colour upon exposure to oxygen for 55 min under ambient conditions (~21 °C, ~55%RH, 21% O<sub>2</sub>). The response sensor was evaluated by a camera based on the measurement of the H colour coordinate as the analytical parameter *versus* % O<sub>2</sub>, always that the indicator is activated, photoreduced, so the initial colour will be white, and in contact with oxygen, oxidation will occur, and the indicator colour will be blue. The results obtained show that the sensor is stable during the time that it is not in contact with oxygen. Relative humidity greater than 60% significantly affects the re-oxidation process, and the temperature has a significant influence on the colour recovery, although the stability increases considerably when the sensor is kept refrigerated at 4 °C. A real application to packaged ham was carried out, demonstrating that the sensor has the capacity to forecast the end of life of the food and that it could be used as an oxygen indicator in intelligent packaging for foods that are sensitive to oxidation. It is possible to find out the oxygen content by taking a photograph of the sensor and whether the tightness of the container is compromised by simply observing the colour of the membrane.

## Author contributions

M.D. F-R. and I.M. P-S. designed research; M.P-R. and M.D. F-R. and I.M. P-S. performed research; M.D.F-R., I.M. P-S and L.F. C-V. analyzed data; and M.D. F-R and L.F. C-V. wrote the paper.

## Conflicts of interest

The authors declare that they have no known competing financial interests or personal relationships that could have appeared to influence the work reported in this paper.

## Acknowledgements

This study was supported by the Spanish Ministerio de Economía y Competitividad (Projects PID2019-103938RB-I00 and CTQ2017-86125-P) and Junta de Andalucía (Projects B-FQM-243-UGR18 and P18-RT-2961). The projects were par-

tially supported by European Regional Development Funds (ERDF).

## References

- 1 S. Kalpana, S. R. Priyadarshini, M. Maria Leena, J. A. Moses and C. Anandharamakrishnan, *Trends Food Sci. Technol.*, 2019, **93**, 145–157.
- 2 E. Poyatos-Racionero, J. V. Ros-Lis, J.-L. Vivancos and R. Martínez-Mañez, *J. Cleaner Prod.*, 2018, **172**, 3398–3409.
- 3 A. L. Brody, E. P. Strupinsky and L. R. Kline, *Active Packaging for Food Applications*, CRC Press, 2019.
- 4 M. L. Rooney, *Active Food Packaging*, Springer US, 1995.
- 5 K. B. Biji, C. N. Ravishankar, C. O. Mohan and T. K. Srinivasa Gopal, *J. Food Sci. Technol.*, 2015, **52**, 6125–6135.
- 6 A. Mills, *Chem. Soc. Rev.*, 2005, **34**, 1003–1011.
- 7 Z. Zhujun and W. R. Seitz, *Anal. Chem.*, 1986, **58**, 220–222.
- 8 K. E. Chung, E. H. Lan, M. S. Davidson, B. S. Dunn, J. S. Valentine and J. I. Zink, *Anal. Chem.*, 1995, **67**, 1505–1509.
- 9 A. Del Bianco, F. Baldini, M. Bacci, I. Klimant and O. S. Wolfbeis, *Sens. Actuators, B*, 1993, **11**, 347–350.
- 10 Z. Fang, Y. Zhao, R. D. Warner and S. K. Johnson, *Trends Food Sci. Technol.*, 2017, **61**, 60–71.
- 11 G. López-Carballo, V. Murial-Galet, P. Hernández-Muñoz and R. Gavara, *Sensors*, 2019, **19**, 4684–4697.
- 12 S.-K. Lee, M. Sheridan and A. Mills, *Chem. Mater.*, 2005, **17**, 2744–2751.
- 13 P. Marek, J. J. Velasco-Veléz, T. Haas, T. Doll and G. Sadowski, *Sens. Actuators, B*, 2013, **178**, 254–262.
- 14 A. Mills and D. Hazafy, *Analyst*, 2008, **133**, 213–218.
- 15 A. Mills and D. Hazafy, *Sens. Actuators, B*, 2009, **136**, 344–349.
- 16 A. Mills and K. Lawrie, *Sens. Actuators, B*, 2011, **157**, 600–605.
- 17 E. J. Son, J. S. Lee, M. Lee, C. H. T. Vu, H. Lee, K. Won and C. B. Park, *Sens. Actuators, B*, 2015, **213**, 322–328.
- 18 C. H. T. Vu and K. Won, *Food Chem.*, 2013, **140**, 52–56.
- 19 C. H. T. Vu and K. Won, *J. Agric. Food Chem.*, 2014, **62**, 7263–7267.
- 20 S. Khankaew, A. Mills, D. Yusufu, N. Wells, S. Hodgen, W. Boonsupthip and P. Suppakul, *Sens. Actuators, B*, 2017, **238**, 76–82.
- 21 A. Mills, K. Lawrie, J. Bardin, A. Apedaile, G. A. Skinner and C. O'Rourke, *Analyst*, 2012, **137**, 106–112.
- 22 K. Lawrie, A. Mills and D. Hazafy, *Sens. Actuators, B*, 2013, **176**, 1154–1159.
- 23 S. Magdassi, *The Chemistry of Inkjet Inks*, 2009.
- 24 D. W. Peter and K. K. Tobias, *Analyst*, 2005, **130**, 1331–1336.
- 25 M. Quaranta, S. M. Borisov and I. Klimant, *Bioanal. Rev.*, 2012, **4**, 115–157.



- 26 V. B. Llorente, E. M. Erro, A. M. Baruzzi and R. A. Iglesias, *Sens. Actuators, B*, 2015, **216**, 316–320.
- 27 H. Golnabi and M. Razani, *Sens. Actuators, B*, 2007, **122**, 109–117.
- 28 P. G. Tratnyek, T. E. Reilkoff, A. W. Lemon, M. M. Scherer, B. A. Balko, L. M. Feik and B. D. Henegar, *Chem. Educ.*, 2001, **6**, 172–179.
- 29 D. Ollis, A. Mills and K. Lawrie, *Appl. Catal., B*, 2016, **184**, 201–207.
- 30 A. Mills and G. A. Skinner, *Analyst*, 2011, **136**, 894–896.
- 31 Y. Galagan and W. F. Su, *J. Photochem. Photobiol., A*, 2008, **195**, 378–383.
- 32 A. Mills, D. Hazafy and K. Lawrie, *Catal. Today*, 2011, **161**, 59–63.

